Semiconductor Physics, Quantum Electronics & Optoelectronics, 2017. V. 20, N 3. P. 369-374.
doi: https://doi.org/10.15407/spqeo20.03.369

PACS 78.40.Ha; 77.80.Bh

Structure and Raman spectra of $(Cu_6PS_5I)_{1-x}(Cu_7PS_6)_x$ mixed crystals

I.P. Studenyak[1], M.M. Luchynets[1], V.Yu. Izai[1], A.I. Pogodin[1], O.P. Kokhan[1], Yu.M. Azhniuk[1,2], D.R.T. Zahn[3]
[1]*Uzhhorod National University, Faculty of Physics,*
3, Narodna Sq., 88000 Uzhhorod, Ukraine
[2]*Institute of Electron Physics, NAS of Ukraine, 88000 Uzhhorod, Ukraine*
[3]*Semiconductor Physics, Chemnitz University of Technology, D-09107 Chemnitz, Germany*
E-mail: studenyak@dr.com

Abstract. Mixed $(Cu_6PS_5I)_{1-x}(Cu_7PS_6)_x$ crystals were grown using a direct crystallization technique. Being based on the X-ray diffraction data, their crystal structure was studied, showing face-centred cubic lattice for Cu_6PS_5I-rich solid solutions ($x < 0.12$) and primitive cubic lattice for Cu_7PS_6-rich ($0.84 < x < 1$) solid solutions. These structural data correlate with the Raman spectra where, besides the common features typical for the argyrodite-type Cu_6PS_5I and Cu_7PS_6 crystals, weaker bands characteristic only for the end-point compounds are revealed in the corresponding compositional intervals.

Keywords: solid electrolytes, mixed crystals, crystal structure, Raman scattering.

Manuscript received 20.05.17; revised version received 10.07.17; accepted for publication 06.09.17; published online 09.10.17.

1. Introduction

Cu_6PS_5I and Cu_7PS_6 compounds are solid electrolytes of the argyrodite family [1, 2]. At room temperature, they crystallize in the cubic crystal system ($F\bar{4}3m$ and $P2_13$ space groups, respectively). While Cu_6PS_5I has been investigated more extensively [3, 4], the studies of Cu_7PS_6 are very scarce [5–7]. At low temperatures, the Cu_6PS_5I crystal undergoes two phase transitions (PTs), one of them being a first-order superionic and ferroelastic PT at T_I = 144–169 K, another is a second-order structural PT at T_{II} = (269±2) K [8, 9].

The phase diagram of a quasi-binary Cu_2S–P_4S_{10} system was studied in [5]. Cu_7PS_6 compound is formed with a large excess of S^{2-} anions, and in a simplified case its structure can be viewed as a Cu_2S matrix containing isolated $[PS_4]^{3-}$ ions. In Cu_7PS_6, PT is observed at 515 K from the high-temperature phase with $F\bar{4}3m$ symmetry to the low-temperature phase with $P2_13$ symmetry. Calorimetric studies of Cu_7PS_6 showed no phase transitions within the temperature range 100 to 400 K, the linear temperature dependence of specific heat capacity being an evidence for strong anharmonicity [6].

In this paper, we report on growth technology, crystal structure and Raman scattering in $(Cu_6PS_5I)_{1-x}(Cu_7PS_6)_x$ mixed crystals.

2. Experimental

$(Cu_6PS_5I)_{1-x}(Cu_7PS_6)_x$ mixed crystals were grown using the direct crystallization technique from the melt (Bridgman–Stockbarger method). Synthesis of $(Cu_6PS_5I)_{1-x}(Cu_7PS_6)_x$ compounds was performed by the following procedure: heating at a rate of 50 K/h to (673 ± 5) K, ageing at this temperature for 24 h, then heating of the "hot" zone to (1330 ± 5) K and the "cold" zone to (973 ± 5) K, ageing at this temperature for 72 h

Semiconductor Physics, Quantum Electronics & Optoelectronics, 2017. V. 20, N 3. P. 369-374.
doi: https://doi.org/10.15407/spqeo20.03.369

and further heating of the melting zone up to (1380 ± 5) K (50 K above the melting point) with 24 h ageing. Seeding was performed for 48 h in the lower part of the container. The crystallization front rate was 3 mm/day. The ampoule with the crystal was subsequently annealed in the "cold" zone at (973 ± 5) K for 48 h. As a result, $(Cu_6PS_5I)_{1-x}(Cu_7PS_6)_x$ single crystals with the length 45–50 mm and diameter 10–12 mm were obtained.

Based on the experimental X-ray diffraction data, measured using a DRON 4-07 diffractometer, the atom coordinates in the $(Cu_6PS_5I)_{1-x}(Cu_7PS_6)_x$ mixed crystal cells were obtained, and the mechanism of the S→I substitution was clarified. The calculations were performed using EXPO 2014 software [10, 11].

Micro-Raman studies were performed at room temperature using a Horiba LabRAM spectrometer with a CCD camera and a 632.8 nm He-Ne laser. The spectral resolution was better than 2.5 cm^{-1}.

3. Results and discussion

Typical examples of X-ray diffraction patterns of the $(Cu_6PS_5I)_{1-x}(Cu_7PS_6)_x$ solid solutions are shown in Fig. 1. Based on the X-ray diffraction data, the crystalline structure of the mixed crystals of Cu_6PS_5I–Cu_7PS_6 system was built based on adjusted models of the initial structures using the well-known Rietveld refinement method [12, 13]. Cu_6PS_5I compound crystallizes in the face-centred cubic cell ($F\bar{4}3m$ space group, a = 9.736(1) Å, the number of formula units Z = 4) [1].The structure is formed by $[PS_4]$, $[S_3I]$, and $[SI_4]$ tetrahedra, on the faces and in the middle of which copper atoms are located (Fig. 2a). For Cu_6PS_5I, the $[PS_4]$ tetrahedron is symmetrical (Fig. 2b) with S2–S2 distance of 3.351 Å and P–S2 distance of 2.052 Å, its volume being calculated as 4.44 $Å^3$.

Copper atoms in the Cu_6PS_5I structure are distributed over nearly equivalent positions of two kinds Cu1 and Cu2 (24 h and 48 g Wyckoff positions). Hopping of copper atoms between these positions is the factor responsible for the ionic conductivity of Cu_6PS_5I [1-4]. The conductivity is determined by triangularly coordinated Cu1 copper atoms located in the center of CuS_3I_2 doubled tetrahedra.

In the Cu_7PS_6 structure ($P2_13$ space group), the anion core is formed by four kinds of sulphur atoms (Fig. 3a), the $[PS_4]$ tetrahedra are distorted (Fig. 3b). The phosphorus atom is displaced towards the S2S2S2 plane and the S–S distances are not equal: the S2–S2 distance is 3.395 Å, the S2–S3 is 3.251 Å). The P–S distances for the two kinds of sulphur atoms are 2.029 Å (P–S2), 2.068 Å (P–S3). The $[PS_4]$ tetrahedron volume for this structure is 4.31 $Å^3$.

For mixed $(Cu_6PS_5I)_{1-x}(Cu_7PS_6)_x$ crystals, it is essential to consider separately Cu_6PS_5I-rich and Cu_7PS_6-rich compounds, since from our recent study [7] it follows that $(Cu_6PS_5I)_{1-x}(Cu_7PS_6)_x$ solid solutions do not form a continuous compositional row, existing only in the $0 < x < 0.12$ and $0.84 < x < 1$ intervals. Due to the eutectic type of interaction in the Cu_6PS_5I–Cu_7PS_6 system (with the $x = 0.3$ eutectic point coordinate), the intermediate range ($0.12 < x < 0.84$) corresponds to the coexistence of these two phases.

For Cu_6PS_5I-rich solid solutions ($0 < x < 0.12$), the S3 (4a) sulphur atoms are substituted by iodine atoms without displacement (Fig. 4a). The $[PS_4]$ tetrahedron (Fig. 4b), similarly to Cu_6PS_5I, remains symmetrical with the S2–S2 distances of 3.267 Å, the P–S2 distances of 2.001 Å, and the tetrahedron volume of 4.11 $Å^3$. The data were calculated for the $(Cu_6PS_5I)_{0.9}(Cu_7PS_6)_{0.1}$ compound.

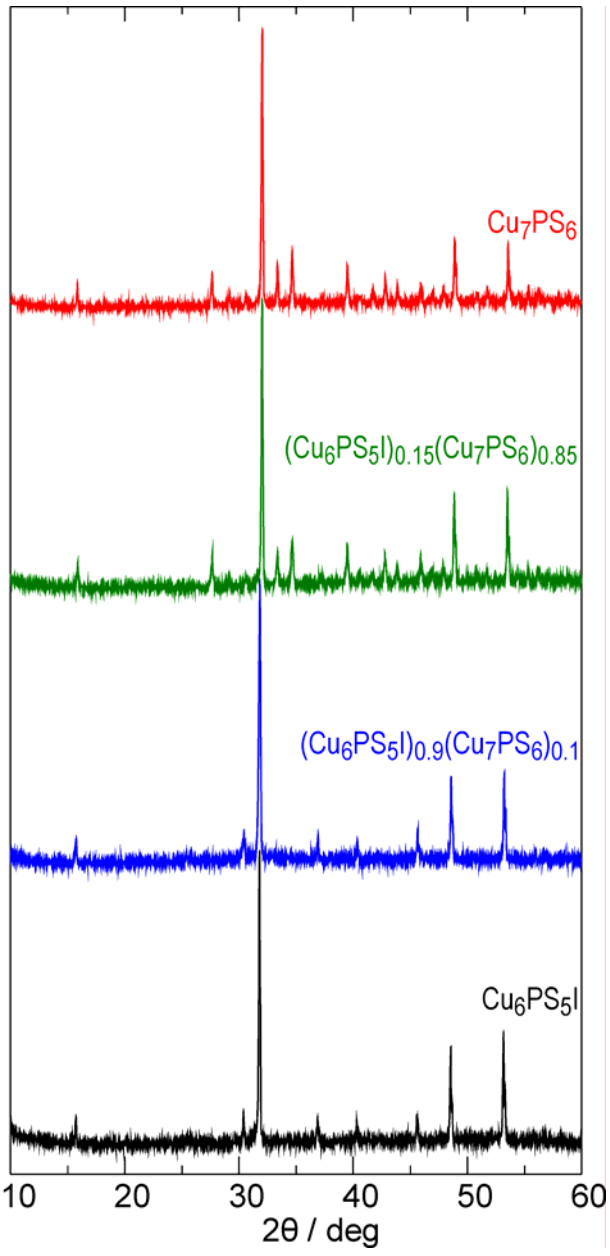

Fig. 1. X-ray diffraction patterns of the $(Cu_6PS_5I)_{1-x}(Cu_7PS_6)_x$ mixed crystals.

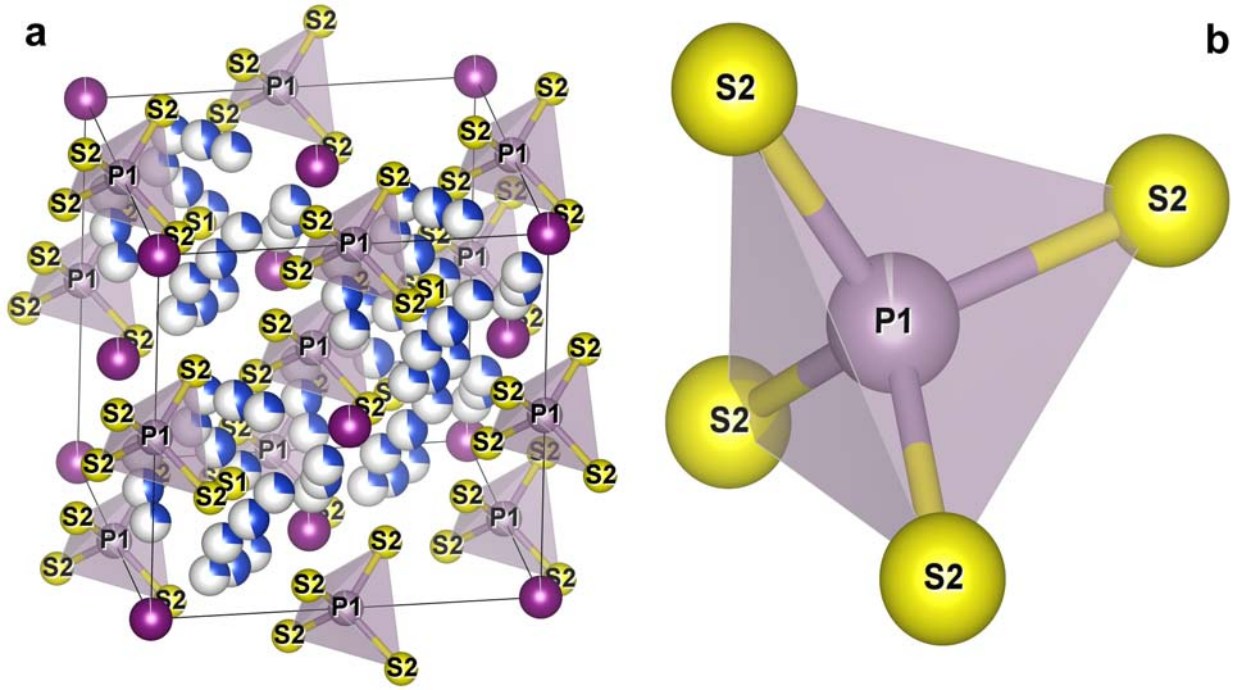

Fig. 2. Structure of the cubic cell (a) and the [PS_4] tetrahedron (b) for Cu_6PS_5I. Violet circles denote iodine atoms, while blue-and-white circles denote the nearly equivalent positions of copper atoms, the extent of the blue colour corresponding to the site occupancy.

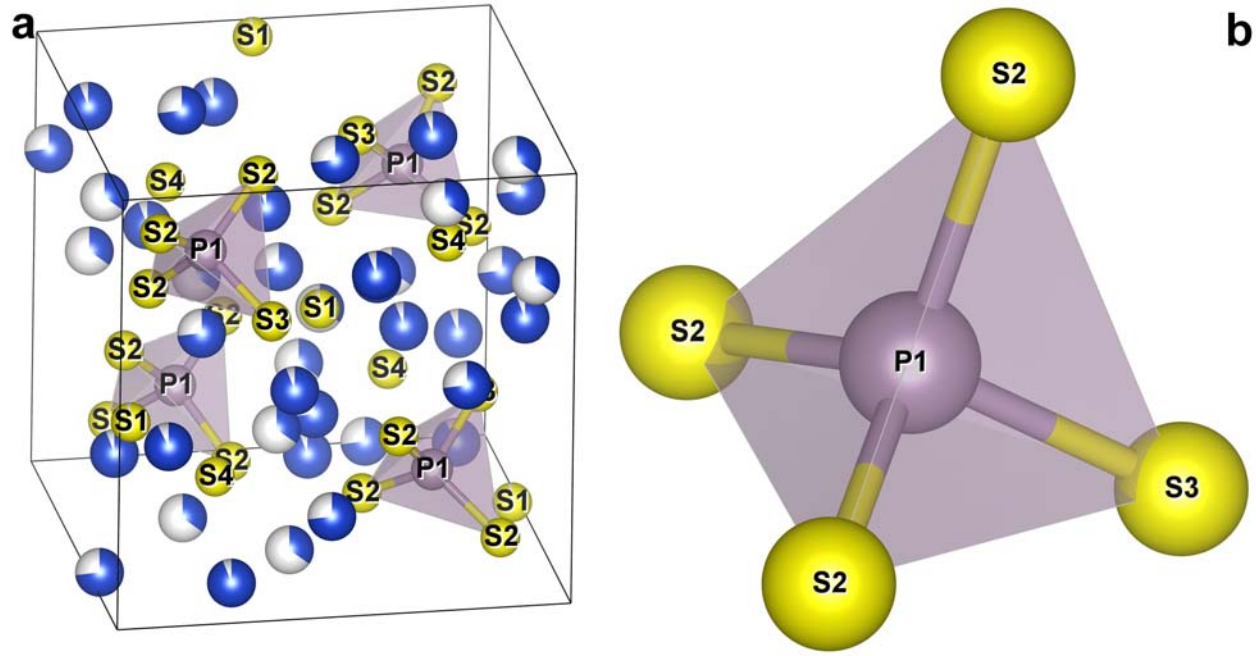

Fig. 3. Structure of the cubic cell (a) and the [PS_4] tetrahedron (b) for Cu_7PS_6. Blue-and-white circles denote the nearly equivalent positions of copper atoms, the extent of the blue colour corresponding to the site occupancy.

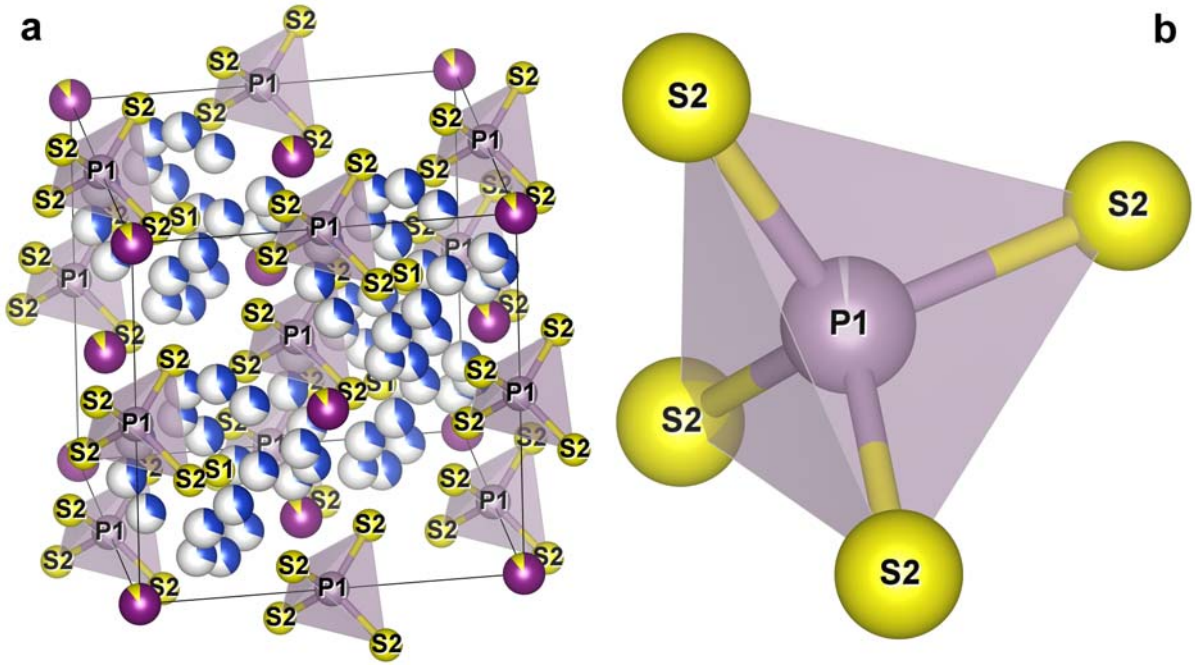

Fig. 4. Structure of the cubic cell (a) and the [PS_4] tetrahedron (b) for $(Cu_6PS_5I)_{0.9}(Cu_7PS_6)_{0.1}$. Violet circles denote iodine atoms while blue-and-white circles denote the nearly equivalent positions of copper atoms, the extent of the blue colour corresponds to the site occupancy.

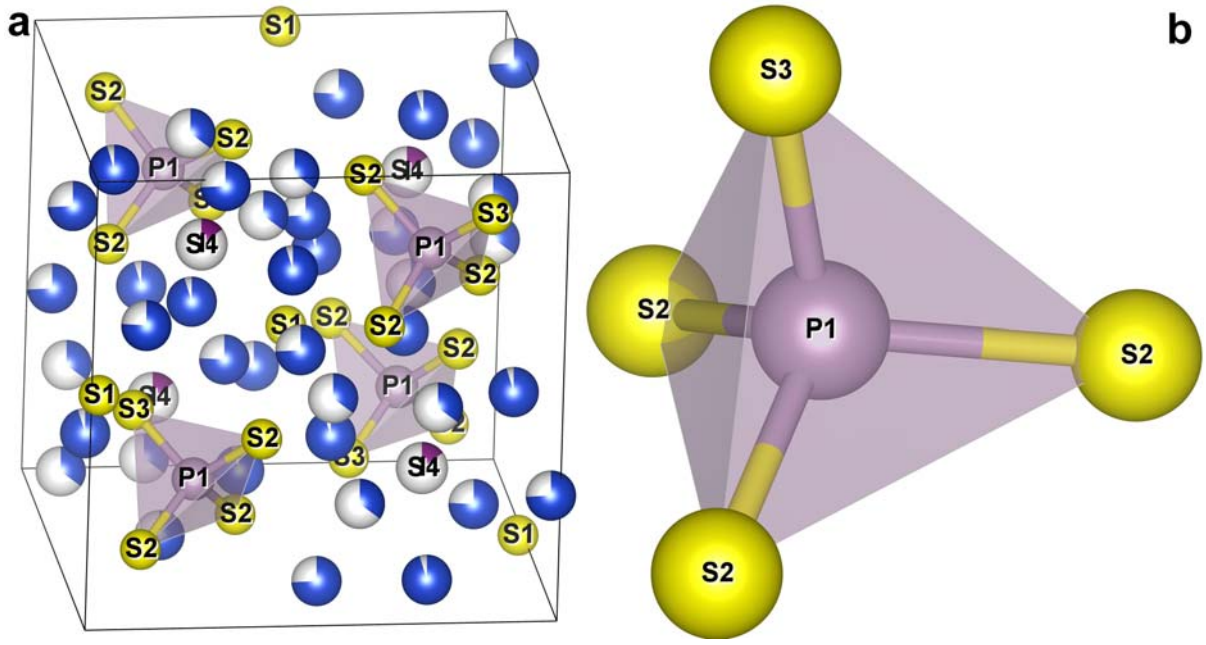

Fig. 5. Structure of the cubic cell (a) and the [PS_4] tetrahedron (b) for $(Cu_6PS_5I)_{0.15}(Cu_7PS_6)_{0.85}$. Blue-and-white circles denote the nearly equivalent positions of copper atoms, the extent of the blue colour corresponds to the site occupancy. White S4 circles are partly coloured violet denoting partial substitution with iodine.

For the Cu_7PS_6-rich solid solutions (the compositional range $0.84 < x < 1$) with $P2_13$ structure, sulphur is replaced with iodine in the S4 (4a) positions. For the nearly limiting case of $(Cu_6PS_5I)_{0.15}(Cu_7PS_6)_{0.85}$, the [$PS_4$] tetrahedron is distorted due to the asymmetry of the S–S bonds (the S2–S2 distance is 3.347 Å, the S2–S3 one is 3.194 Å) and a displacement of the phosphorus atom towards the S2S2S2 plane (Fig. 5). The corresponddding P–S distances are 2.029 Å (P–S2) and 1.923 Å (P–S3), the [PS_4] tetrahedron volume is 4.11 Å.

Despite the great number of atoms in the unit cell, the room-temperature Raman spectrum of Cu_6PS_5I

single crystal (the bottom curve in Fig. 6) is known to contain a relatively small number of vibrational bands [14], which can be related to the fact that some of them, being close in frequency, can be resolved only at lower temperatures. Besides, the lower-frequency bands corresponding to the vibrations of more weakly bound iodine and copper atoms can be masked by the Rayleigh scattering tail. The dominating feature is a narrow (7 cm^{-1}) peak at 420 cm^{-1} corresponding to a symmetric vibration of the PS_4 tetrahedra. A less intense, much broader (39 cm^{-1}) peak at 308 cm^{-1} results from the unresolved degenerated E and F_2 bands assigned to bending vibrations of the PS_4 tetrahedral groups [14, 15]. A weaker band observed at 539 cm^{-1} is ascribed to internal stretching vibrations of the PS_4 tetrahedra [14].

As can be seen from the topmost curve in Fig. 6, for Cu_7PS_6 the Raman spectrum resembles that of Cu_6PS_5I, with a similar dominating narrow (6 cm^{-1}) peak at 425 cm^{-1} and a broader (50 cm^{-1}) maximum at 303 cm^{-1}. Since these two compounds are of basically similar argyrodite structure with the same PS_4 tetrahedral groups, we, similarly to Cu_6PS_5I [14], can assign the maxima at 425 and 303 cm^{-1} in the Raman spectrum of Cu_7PS_6 to the symmetric stretching vibrations of the PS_4 tetrahedra and their bending vibrations, respectively.

However, there are distinct features that noticeably distinguish the Cu_7PS_6 spectrum from that of Cu_6PS_5I. A clear lower-frequency maximum is observed at 142 cm^{-1} as well as a relatively weak shoulder is resolved at 227 cm^{-1} (see the topmost curve in Fig. 6). There are no data regarding any features at close frequencies for the Raman spectra of Cu_6PS_5I, Cu_6PS_5Br or Cu_6PS_5Cl crystals although some weak maxima in the range 100–200 cm^{-1} were reported [14]. Their nature cannot be clearly specified yet, most likely these bands cannot be related to the internal vibrations of the PS_4 tetrahedra. With regard to the weaker high-frequency band observed at 539 cm^{-1} for Cu_6PS_5I, there is no evidence for a similar maximum in the Raman spectrum of Cu_7PS_6. One should note that Cu_7PS_6 is characterized by a primitive cubic crystal lattice ($P2_13$ space group), contrary to the face-centred cubic lattice for Cu_6PS_5I ($F\bar{4}3m$), which can be the reason for absence of the corresponding vibration in the Cu_7PS_6 spectrum.

The evolution of Raman spectra of the mixed $(Cu_6PS_5I)_{1-x}(Cu_7PS_6)_x$ crystal samples with x can be traced from Fig. 6. For Cu_7PS_6-rich samples with $x = 0.85$ and $x = 0.90$ the spectra are very much like to that of Cu_7PS_6, with the clearly visible peak near 143 cm^{-1} and weak shoulder near 225 cm^{-1}, and without any pronounced features around near 540 cm^{-1}. Such behaviour is consistent with the existence of a continuous row of crystalline solid solutions in this compositional range ($0.84 < x < 1$) with $P2_13$ structure. Meanwhile, with further increasing the Cu_6PS_5I content (decreasing x) in the Raman spectra of the solid solutions, one can observe a maximum in the range 530–540 cm^{-1}, while the features near 143 and 225 cm^{-1} vanish. It correlates with the data of the structural studies [7] showing that in the broad intermediate range the Cu_7PS_6-like phase of the $P2_13$ structure coexists with the Cu_6PS_5I-like phase of the $F\bar{4}3m$ symmetry group, and the features typical for the latter are revealed in the Raman spectra.

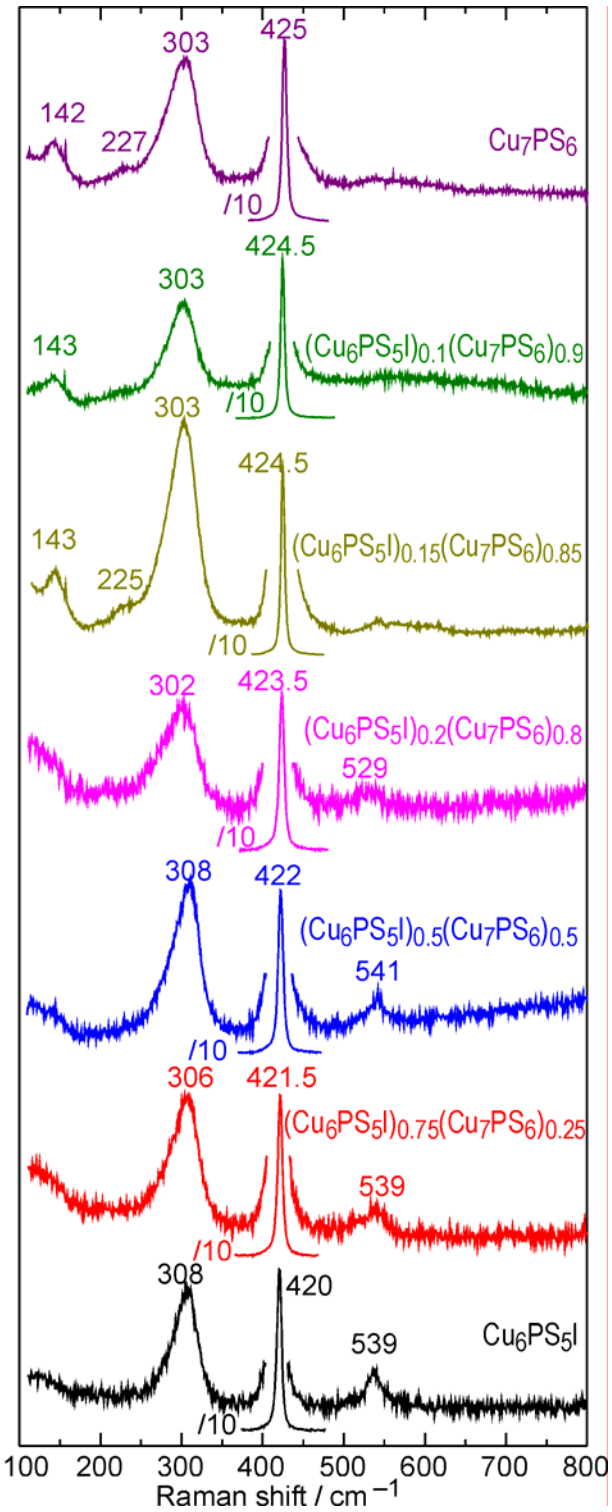

Fig. 6. Room-temperature Raman spectra of $(Cu_6PS_5I)_{1-x}(Cu_7PS_6)_x$ crystals measured under the excitation with $\lambda_{exc} = 632.8$ nm.

4. Conclusions

Mixed $(Cu_6PS_5I)_{1-x}(Cu_7PS_6)_x$ crystals were grown using the direct crystallization technique. Based on the X-ray diffraction data, their crystal structure has been studied, showing face-centred cubic lattice for Cu_6PS_5I-rich solid solutions ($x < 0.12$) and primitive cubic lattice for Cu_7PS_6-rich ($0.84 < x < 1$) solid solutions. This change of the lattice structure with the heterovalent S→I substitution occurs due to a distortion of the $[PS_4]$ tetrahedron.

Despite the basic similarity of the Raman spectra of the argyrodite-type Cu_6PS_5I and Cu_7PS_6 crystals, relatively weak bands typical only for Cu_6PS_5I (539 cm^{-1}) and Cu_7PS_6 (143 and 226 cm^{-1}) end-point compounds have been revealed. The maxima at 143 and 226 cm^{-1} have been also observed for the mixed $(Cu_6PS_5I)_{1-x}(Cu_7PS_6)_x$ crystals of the Cu_7PS_6-rich compositional interval ($0.84 < x < 1$), which, together with the absence of the high-frequency band at 539 cm^{-1}, clearly correlates with the $P2_13$ structure of the Cu_7PS_6-rich phase. The band at 539 cm^{-1} observed for the intermediate $(Cu_6PS_5I)_{1-x}(Cu_7PS_6)_x$ compositional range with the coexisting $P2_13$ and $F\bar{4}3m$ phases correlates with the Cu_6PS_5I-type face-centred structure.

References

1. Kuhs W.F., Nitsche R., Scheunemann K. Vapour growth and lattice data of new compounds with icosahedral structure of the type Cu_6PS_5Hal (Hal=Cl, Br, I). *Mat. Res. Bull*. 1976. **11**. P. 1115–1124.
2. Kuhs W.F., Nitsche R., Scheunemann K. The argyrodites – a new family of the tetrahedrally close-packed structures. *Mat. Res. Bull*. 1979. **14**. P. 241–248.
3. Studenyak I.P., Kranjčec M. *Disordering Effects in Superionic Conductors with Argyrodite Structure*. Uzhhorod: Hoverla, 2007 (in Ukrainian).
4. Studenyak I.P., Kus P. *Structural Disorder in Crystalline and Amorphous Superionic Conductors*. Uzhhorod: Hoverla, 2016.
5. Andrae H., Blachnik R. Metal sulphide-tetraphosphorusdecasulphide phase diagrams. *J. Alloys and Compounds*. 1992. **189**. P. 209–215.
6. Fiechter S., Gmelin E. Thermochemical data and phase transition of argyrodite-type ionic conductors Me_6PS_5Hal and Me_7PS_6 (Me = Cu, Ag; Hal = Cl, Br, I). *Thermochimica Acta*. 1985. **87**. P. 319–334.
7. Pogodin A.I., Barchiy I.E., Kokhan A.P. The Cu_2S–Cu_7PS_6–Cu_6PS_5I quasi-ternary system. *Chem. Met. Alloys*. 2013. **6**. P. 188-191.
8. Studenyak I.P., Kranjčec M., Kovacs Gy.Sh., Panko V.V., Mitrovcij V.V., Mikajlo O.A. Structural disordering studies in $Cu_{6+\delta}PS_5I$ single crystals. *Mater. Sci. Eng*. 2003. **B97**. P. 34–38.
9. Gagor A., Pietraszko A., Kaynts D. Diffusion paths formation for Cu^+ ions in superionic Cu_6PS_5I single crystals studied in terms of structural phase transition. *J. Solid State Chem*. 2005. **178**. P. 3366–3375.
10. Altomare A., Burla M.C., Camalli M., Carrozzini B., Cascarano G., Giacovazzo C., Guagliardi A., Moliterni A.G.G., Polidori G., Rizzi R. EXPO: a program for full powder pattern decomposition and crystal structure solution. *J. Appl. Crystallogr*. 1999. **32**. P. 339–340.
11. Altomare A., Cuocci C., Giacovazzo C., Moliterni A., Rizzi R., Corriero N., Falcicchio A. EXPO2013: a kit of tools for phasing crystal structures from powder data. *J. Appl. Crystallogr*. 2013. **46**. P. 1231–1235.
12. Rietveld H.M. A profile refinement method for nuclear and magnetic structures. *J. Appl. Crystallogr*. 1969. **2**. P. 65–71.
13. McCusker L.B., Von Dreele R.B., Cox D.E., Louër D., Scardi P. Rietveld refinement guidelines. *J. Appl. Crystallogr*. 1999. **32**. P. 36–50.
14. Studenyak I.P., Stefanovich V.O., Kranjcec M., Desnica D.I., Azhnyuk Yu.M., Kovacs Gy.Sh., Panko V.V. Raman scattering studies of Cu_6PS_5Hal (Hal = Cl, Br, I) fast-ion conductors. *Solid State Ionics*. 1997. **95**. P.221–225.
15. Kranjčec M., Studenyak I.P., Buchuk R.Yu., Stephanovich V.O., Kökényesi S., Kis-Varga M. Structural properties and Raman scattering in Cu_6PS_5X (X = I, Br) nanocrystalline solid electrolytes. *Solid State Ionics*. 2008. **179**. P.218–221.